Isolation of the Improved Core Confinement from High Recycling and Radiative Boundary in Reversed Magnetic Shear Plasmas of JT-60U

K. Itami, R. Yoshino, N. Asakura, T. Fujita, N. Hosogane, O. Naito, S. Higashijima, S. Konoshima, A. Sakasai, H. Takenaga, and M. Shimada

Japan Atomic Energy Research Institute, Naka Fusion Research Establishment, Naka-machi, Naka-gun, Ibaraki-ken, 311-01, Japan

(Received 19 September 1996)

Isolation of the core with improved confinement (inside the internal transport barrier) from high recycling and strongly radiative boundary plasmas was demonstrated for the first time in the reversed shear plasmas of the JT-60U tokamak. The internal transport barrier remained intact, while edge radiation and recycling was enhanced with neon and hydrogen gas puffing. The internal transport barrier reduced the particle transport by a factor 10–15, while shrinking in the time scale of resistive diffusion towards the center. [S0031-9007(97)02412-5]

PACS numbers: 52.55.Fa

One of the most difficult requirements in the fusion reactor is to achieve high temperature in the core plasma and low temperature in the boundary plasma at the same time. Low recycling of neutral particles in the edge facilitates confinement improvement [1,2], but it causes low density and high temperature plasma in the divertor and high heat flux density to the divertor targets [3].

The improved core plasma confinement inside the internal transport barrier, recently produced in reversed magnetic shear discharges, shows plasma performance attractive for fusion reactors [4–6]. In reversed magnetic shear plasmas, it is possible to operate with L-mode profiles outside the transport barriers. L-mode edge confinement is compatible with high particle recycling conditions in the scrape-off layer (SOL) and divertor plasma, which can effectively promote the radiative divertor plasma. Here the radiative divertor is the idea of dissipating a large fraction of heat flux by radiative cooling of the dense and cold divertor plasma [7]. Thus if it is possible to isolate the internal transport barrier from high recycling SOL and radiative divertor plasmas, the reversed shear plasma becomes a promising scheme for a fusion reactor. Recent radiative divertor experiments in JT-60U have addressed this issue, as described in this Letter.

In JT-60U, significant reduction in thermal diffusivities of both ions and electrons has been observed at the internal transport barrier (ITB) in the reversed magnetic shear plasmas [6]. The internal transport barrier, which is characterized by the steep gradient of the ion temperature T_i, electron temperature T_e, and electron density n_e, typically appears at $r/a = \sim 0.4$–0.65 in the negative magnetic shear region. The ratio of T_i to T_e inside the ITB can be lower than 1.5, when a deuterium or hydrogen gas puff is applied during the start-up phase of the discharges.

Neon and hydrogen gas injection were applied to a series of the reversed shear plasmas after the formation of the transport barrier. It has been demonstrated in the limiter discharges [8] and then in the divertor experiments [9,10] that a small amount of neon injection enhanced the total radiation loss up to 80%–95% of the input power without degrading confinement in the main plasmas. The discharges were hydrogen plasmas with the plasma current $I_P = 1.2$ MA, toroidal field $B_T = 3.4$ T, and the neutral beam power $P_{\mathrm{NBI}} = 13.5$ MW of hydrogen beams. The major radius, minor radius, and ellipticity of the plasmas were $R = 3.4$ m, $a = 0.88$ m, and $\kappa = 1.47$, respectively.

The preheating beam power and the plasma configuration were programmed to be identical and the density feedback was employed so that the line-averaged density of the central chord ($r/a = 0.16$) $\overline{n}_e$ traced the preprogrammed value during the I_P ramp-up phase in this series of discharges. Combination of a pulsed neon puff and a hydrogen puff with density feedback control to the optimum $\overline{n}_e$ resulted in sustainment of the internal transport barrier for as long as one second, along with a strongly radiative divertor, as shown in Fig. 1(a). In this discharge, the internal transport barrier started to develop at $t = 5.1$ s with main beam heating of $P_{\mathrm{NBI}} = 13.5$ MW. A neon puff was applied at $t = 5.5$ s. Line intensity of Ne X shows that the neon content reached a saturation level at $t = 6.0$ s and was sustained for the rest of the discharge. An additional hydrogen puff was applied at $t = 6.5$ s by the density feedback system to ramp up $\overline{n}_e$ to 3.3×10^{19} m^{-3} at $t = 6.8$ s and then to sustain the density until the end of the beam heating.

The increase in radiation loss dominantly originated around the X-point at 20 cm above the divertor plates. $P_{\mathrm{rad}}^{\mathrm{div}}$ reached 7.6 MW during the radiative divertor phase, a factor of 5 increase from 1.4 MW at $t = 5.5$ s, while $P_{\mathrm{rad}}^{\mathrm{main}}$ increased only from 0.4 to 1 MW. Here $P_{\mathrm{rad}}^{\mathrm{div}}$ and $P_{\mathrm{rad}}^{\mathrm{main}}$ are radiation loss from the divertor and X-point and the radiation loss from the main plasma, respectively. This small increase in $P_{\mathrm{rad}}^{\mathrm{main}}$ is a feature much different from the neon puff experiment in ELMy H-mode plasmas, in which a large fraction of radiation loss, typically 30% of beam power, originates from the main plasma [10,11]. This

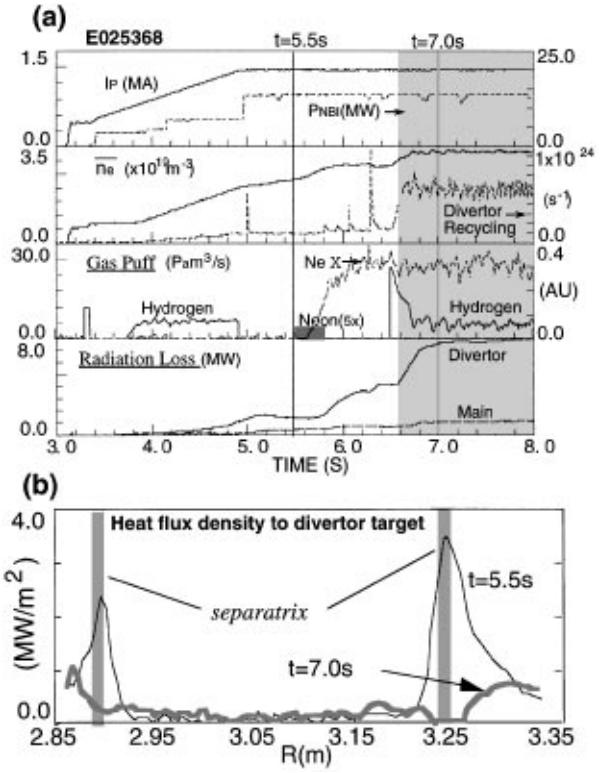

FIG. 1. Time traces of the plasma parameters in shot 25368, a typical reversed magnetic shear plasma with radiative divertor by neon and hydrogen gas puffing. Neon puff rate is multiplied by a factor of 5. (b) Heat flux density profiles measured by an infrared camera before and during the radiative phase in shot 25368.

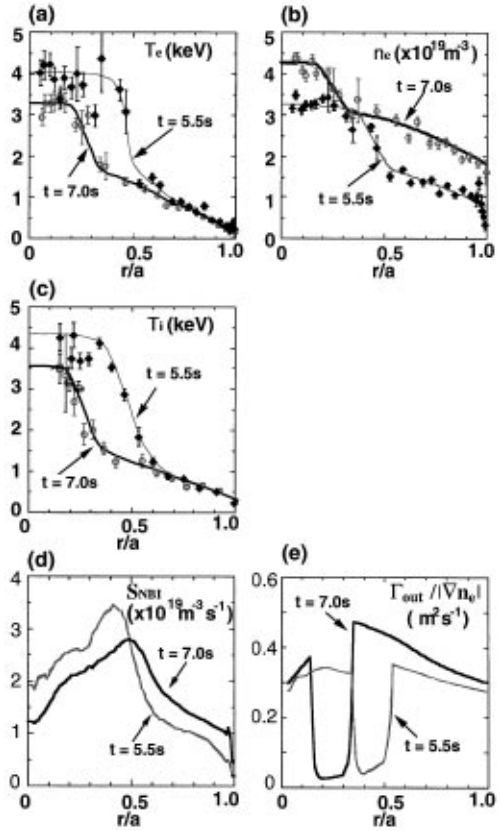

FIG. 2. The following profiles are taken at the time of before ($t = 5.5$ s) and during ($t = 7.0$ s) the radiative divertor phase. (a) Electron temperature profiles measured by Thomson scattering. (b) Electron density profiles measured by Thomson scattering. (c) Ion temperature profiles measured from C^{5+} with the CXRS system. Ion temperature at three channels in the center was measured from Ne^{9+} with another CXRS system at $t = 7.0$ s, as is marked by open square symbols. (d) Profiles of particle source by neutral beams calculated by the TOPICS code. (e) Profiles of $\Gamma_{\text{out}} |\nabla n_e|$.

small increase in the main plasma radiation is consistent with the small increase in Z_{eff} ($\delta Z_{\text{eff}} < 0.3$) over the main plasma. The spectroscopic measurement has shown that the dominant impurities were carbon and oxygen at $t = 5.5$ s. A large fraction of these intrinsic impurities was replaced by neon in the radiative divertor phase. The content of neon was 1.8% of the electron density at $t = 7.0$ s, while oxygen and carbon were reduced from 1.7% to 0.1% and from 3.4% to 1.0%, respectively.

The total radiation loss increased from 16% to 69% of the absorbed beam power. Heat flux to the divertor, measured by an infrared camera, vanished at the strike point of the separatrix as shown in Fig. 1(b), and this detached state was sustained during the radiative divertor phase. The total heat load integrated over the divertor target decreased to 20% of the total input power. The sum of radiation power loss and heat flux to the divertor accounted for ~85%–90% of the absorbed power before and during the radiative divertor phase. Langmuir probe measurement has shown that the particle flux also vanished at the separatrix hit points.

The profiles of electron density, temperature, and ion temperature of the main plasma before ($t = 5.5$ s) and during ($t = 7.0$ s) the radiative divertor phase are shown in Figs. 2(a), 2(b), and 2(c). Ion temperature was routinely measured from C^{5+} by the charge exchange recombination spectroscopy (CXRS) system. Ion temperature at the three channels in the center was measured from Ne^{9+} by another CXRS system at $t = 7.0$ s, since C^{5+} intensity was too low. While the radial position moved inward from $0.4 \leq r/a \leq 0.5$ to $0.2 \leq r/a \leq 0.3$, the steep gradient in n_e, T_e, and T_i profiles survived even in the radiative divertor phases.

The electron temperature was unchanged at $r/a \geq 0.7$, while the electron density increased by a factor of 2. This observation is partly explained by the fact that the effective heating power in the plasma volume of $r/a \geq 0.7$ was increased after the formation of the radiative divertor plasma. It is estimated tha the deposited beam power increased from 2.3 to 3.4 MW, while the radiation loss increased from 0.2 to 0.5 MW in this volume. It should be noted that the density profile was significantly changed just inside the separatrix. The electron density on the separatrix increased from 3×10^{18} m^{-3} before the gas puff to 1.6×10^{19} m^{-3} during the gas puff as

shown in Fig. 2(b). Therefore recycling neutral particles were mostly shielded by the SOL plasma and the charge exchange loss was negligible.

Improvement of particle transport at the internal transport barrier was preserved in the radiative divertor phase. This was confirmed by the reduction of the parameter $\Gamma_{\text{out}}/|\nabla n_e|$ at the transport barrier. Here Γ_{out} and $|\nabla n_e|$ are the particle outflux density and the plasma density gradient, respectively. The radial profiles of $\Gamma_{\text{out}}/|\nabla n_e|$ before and during the radiative divertor as shown in Fig. 2(e). Γ_{out} is given by the particle balance equation $\Gamma_{\text{out}} = \int (S_{NBI} - \partial n_e/\partial t) dV_P/A_P$. Here A_P is the surface area of the flux surface. We assumed the plasma density increased only inside the transport barrier before the gas puffing in order to estimate $\partial n_e/\partial t$ at $t = 5.5$ s. This assumption is justified because the line-averaged density at the chord of $r/a = 0.84$ didn't increase with time before the neon gas puff. The particle source by neutral beams S_{NBI}, shown in Fig. 2(d), was calculated by the TOPICS code [12], incorporating the measured n_e, T_e, and T_i profiles and $Z_{\text{eff}} = 3$ at $t = 5.5$ s and $t = 7$ s. As the plasma density increased in the region of $r/a > 0.5$, the neutral beam deposition became broader at $t = 7.0$ s. As is shown in Fig. 2(e), $\Gamma_{\text{out}}/|\nabla n_e| \sim 0.04$ m^2/s at the internal transport barrier ($0.4 \leq r/a \leq 0.5$) and $\Gamma_{\text{out}}/|\nabla n_e| \sim 0.3$ m^2/s outside the barrier before the gas puff at $t = 5.5$ s. In the radiative divertor phase at $t = 7.0$ s, $\Gamma_{\text{out}}/|\nabla n_e| \sim 0.03$ m^2/s at the internal transport barrier ($0.2 \leq r/a \leq 0.3$) and $\Gamma_{\text{out}}/|\nabla n_e| \sim 0.3$–$0.45$ m^2/s outside the barrier were obtained. Thus particle transport remained reduced by a factor of 10–15 after the formation of the radiative divertor plasma.

Shrinkage of the internal transport barrier was also observed in the soft x-ray intensity profiles, as shown in Figs. 3(a) and 3(b). Figure 3(b) is a contour plot of soft x-ray intensity in shot 25368. The internal transport barrier is located where contour lines are concentrated in Fig. 3(b), since the plasma pressure gradient is large at the barrier. The radial extent of the internal transport barrier is indicated as shaded lines. Before the radiative divertor phase, the barrier shrank toward the center with repetitive mini collapses after $t = 5.8$ s. During the radiative divertor phase, the barrier shrank in the time scale of the resistive diffusion without mini collapses until a major collapse at $t = 7.6$ s. The resistive diffusion time inside the internal transport barrier, defined by $\tau = \mu_0 \sigma r_b^2/2$, is 2.4 sec for $Z_{\text{eff}} = 3$, $T_e = 3$ keV, and the radius of barrier $r_b = 0.25$ m. This value is compatible with the shrinkage of the barrier during the radiative divertor phase.

It seems that the neon injection did not directly change the time scale of the barrier collapse. Since increases in Z_{eff} and $P_{\text{rad}}^{\text{main}}$ during the radiative divertor phase were small, the conductivity of the plasma (σ) was reduced mainly by reduction of T_e associated with increase in n_e by hydrogen gas puffing. Excessive hydrogen gas puffing during the radiative divertor phase resulted in a faster decay of T_e at the center and the subsequent major collapse of the barrier. The major collapse might be a consequence of the current profile relaxation. In the most recent radiative divertor experiment with deuterium beams, it was measured that reversal of central shear became very shallows and the safety factor in the zone was close to 2 before the major barrier collapse.

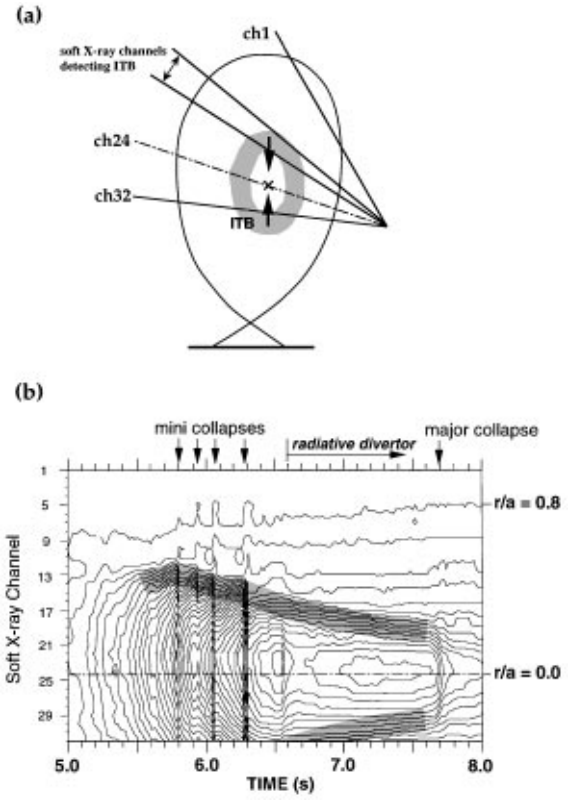

FIG. 3. (a) Radial extent of the internal transport barrier (ITB) is schematically shown with soft x-ray chords. (b) Contour plot reconstructed from the soft x-ray intensity profiles in shot 25368. Shaded lines indicate that he internal transport barrier shrank with time.

While the internal transport barrier is compatible with high particle recycling conditions, reduced recycling level was required during the start-up phase of the discharges to suppress current penetration, allowing deeply reversed magnetic shear, which was required for the barrier formation. The recycling level was controlled by wall conditioning before the discharges. Figure 4(a) shows time traces of $T_e(0.43)$ and $\Phi_{\text{main}}/\overline{n}_e V_p$ in a series of the reversed shear discharges. Here $T_e(0.43)$ is electron temperature just inside the transport barrier ($r/a = 0.43$) from electron-cyclotron emission (ECE) measurement. The recycling level around the main plasma Φ_{main}, measured by a H_α detector array [13], is normalized by the total number of electrons in the main plasma $\overline{n}_e V_p$. V_p is the volume of the main plasma. Shots 25364 and 25368 are distinguished from the other discharges by increases in $T_e(0.43)$ and reductions in $\Phi_{\text{main}}/\overline{n}_e V_p$ due

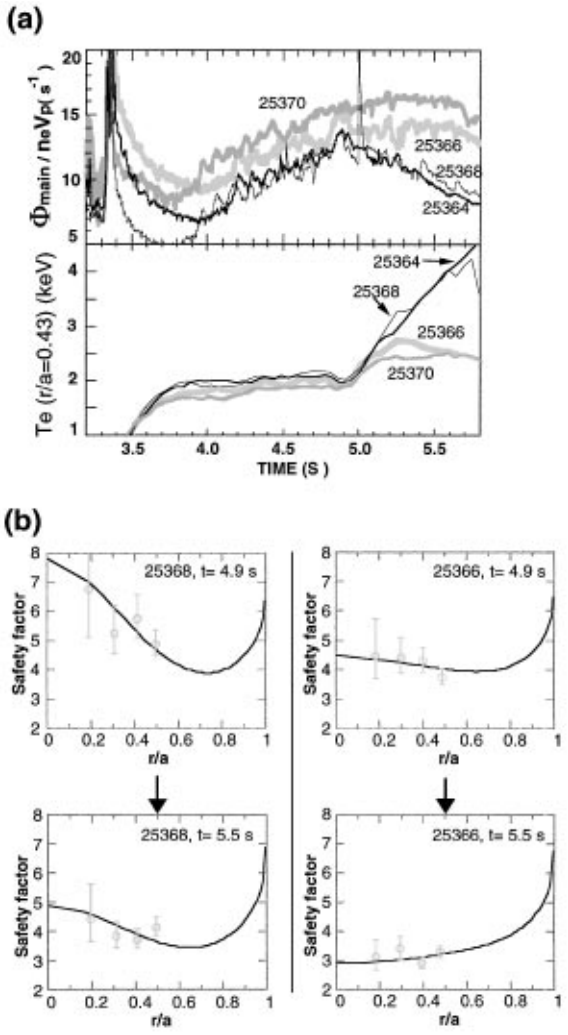

FIG. 4. (a) Time traces of electron temperature at $r/a = 0.43$, just inside the transport barrier, and $\Phi_{\text{main}}/\overline{n}_e V_p$. Shot 25366, in which a recycling level was 20% higher than shots 25364 and 25368, did not develop a transport barrier. (b) Safety factor profiles measured by MSE diagnostics in shots 25368 and 25366 before ($t = 4.9$ s) and during ($t = 5.5$ s) the main beam heating.

to the development of the internal transport barriers after $t = 5.1$ s. These traces also indicate that Φ_{main} was lower in shots 25364 and 25368 than the other discharges, since $\overline{n}_e$ was controlled to the same value by the density feedback before $t = 4.9$ s. Shot 25366 showed slightly lower $T_e(0.43)$ during the I_P ramp-up phase and Φ_{main} larger by 20% than shots 25364 and 25368.

Profiles of safety factor q at the end of the I_P ramp-up ($t = 4.9$ s) and during the main beam heating ($t = 5.5$ s) are compared between shots 25366 and 25368 in Fig. 4(b). These q profiles were obtained by MHD equilibrium analysis using the MSE (motional Stark effect) diagnostics and the value of internal inductance of the plasma [14]. The reversal of the magnetic shear was preserved with the development of the internal transport barrier in shot 25368. In shot 25366 with shallower reversal of the magnetic shear at $t = 4.9$ s, the transport barrier didn't develop and the q profile became monotonic at $t = 5.5$ s. In contrast to such a sensitivity to the recycling level during the start-up phase, the internal transport barrier, once established, was sustained with recycling level increased by a factor of 3 around the main plasma and increased by a factor of 5 in the divertor during the radiative divertor phase in shot 25368.

In the experiment described here, it was demonstrated that the improved core plasma confinement in the reversed shear plasmas was compatible with the high recycling and radiative boundary plasma for the first time in JT-60U. While the internal transport barrier moved inward in the time scale of resistive diffusion, the improvement of the particle confinement, characterized by a factor of 10–15 reduction in $\Gamma_{\text{out}}/|\nabla n_e|$ at the barrier, was maintained even during the radiative divertor phase. This robustness of the internal transport barrier against high recycling and radiative conditions in the boundary plasmas will make reversed shear plasmas attractive for a fusion reactor.

[1] M. Kikuchi *et al.,* in Proceedings of the 14th International Conference on Plasma Physics and Controlled Nuclear Fusion Research, Wurtzburg, 1992 (IAEA, Vienna, 1993), Vol. 1, p. 189.
[2] J. D. Strachan *et al.,* Phys. Rev. Lett. **58**, 1004 (1987).
[3] K. Itami *et al.,* in Ref. [1], Vol. 1, p. 391.
[4] F. M. Levinton *et al.,* Phys. Rev. Lett. **75**, 4417 (1995).
[5] E. J. Strait *et al.,* Phys. Rev. Lett. **75**, 4421 (1995).
[6] T. Fujita *et al.,* Phys. Rev. Lett. (to be published).
[7] M. Shimada *et al.,* Nucl. Fusion **22**, 643 (1982).
[8] U. Samm *et al.,* in Ref. [1], Vol. 1, p. 309.
[9] S. Allen *et al.,* J. Nucl. Mater. **220–222**, 336 (1995).
[10] O. Gruber *et al.,* Phys. Rev. Lett. **74**, 4217 (1995).
[11] K. Itami *et al.,* Plasma Phys. Controlled Fusion **36**, Supplement 11A, A117 (1995).
[12] H. Shirai *et al.,* Proceedings of the 15th International Conference on Plasma Physics and Controlled Nuclear Fusion Research, Seville, 1994 (IAEA, Vienna, 1995), Vol. 1, p. 355.
[13] N. Asakura *et al.,* Nucl. Fusion **35**, 381 (1995).
[14] T. Fujita *et al.,* Fusion Eng. Des. (to be published).